# PIV Investigation on Flows Induced by Fuel Sprays from an Outwards Opening Pintle Injector for GDI engines

Andrea Marchi[1,2], Youyou Yan[1], Jamshid M. Nouri[1] and C Arcoumanis[1]

1: School of Engineering and Mathematical Sciences, City University London, UK
2: Ricardo, Germany

## Abstract

Pintle-type outwards opening injectors actuated by piezoelectric technique have demonstrated the ability to meet the challenging requirements in spray-guided gasoline direct injection engines. Previous studies carried out by spray visualisation showed that the spray had a stable spray cone angle against elevated in-cylinder back pressures, which have been be determined by the integral spray images using continuous or flash white light illumination. However the fuel cloud structure at the end of injection was not well defined when the injection was completed in the white light Mie scattering visualisation. In order to show the details of the spray cloud structure, two dimensional flow visualisation illuminated by a laser sheet was used under the atmospheric condition. The results showed complex multiple vortices forming a recirculation zone inside the fuel cloud. To further study the structure of such vortices, a double pulsed laser sheet illumination was employed to obtain the instantaneous velocity fields of fuel droplets using the Particle Image Velocimetry (PIV) technique. The PIV system was also used to study air motion induced by the spray near the injector nozzle; a good agreement was found in the air entrainment velocities when compared to the LDV measurements.

## Introduction

This experimental work is concerned about the characterisation of the fuel spray structure and of the induced air-entrainment near nozzle exit using a pintle-type injector. Pintle-type outwards opening injectors are actuated by piezoelectric technique and have advantageous features such as the enhanced atomization by high injection pressures up to 200 bar and increased surface contact area between fuel cone spray and the surrounding air; stable spray structures within the range of engine cylinder pressures from the intake stroke to the late compression stroke; and short injection durations comparing to other types of injectors with fast responses at the opening and closing of the pintle valves. The spray exiting the conical ring nozzle of a pintle piezoelectric injector exhibited a string formed hollow conical structure [1-5]. The conical structure is formed by the conical design of the fuel exit passage of the injector. Enlarged injector model tests showed that the string formation on the conical surface is due to either fuel cavitation or air entrainment taking place from outside into the region inside, but close to the injector nozzle exit[6]. Further investigations of spray stabilities were carried out on three prototype injectors operating in a direct injection optical engine by the integral Mie scattering spray visualization [7]. The spray was identified having a stable spray cone angle at the injector nozzle exit and a recirculation zone at the front of the spray. The stability of the spray cone angle was assessed by statistical analysis of the cone angle in terms of the mean cone angle and the standard deviation of the measured cone angles, therefore the stability of injector performances was compared under test conditions including the injection pressure, the in-cylinder backpressure, the injector needle lift and the engine speed. In this paper, the spray cloud structure after the end of injection was investigated by the two-dimensional Mie scattering imaging and the PIV technique; also air motion induced by the spray was measured by both PIV and LDV techniques under the atmospheric condition.

## Experimental Setup

The experiment was carried out in atmosphere using the fuel injection system equipped with a constant volume chamber[1]. A pintle-type outwards opening injector was connected to a common rail. A three-piston-type pump driven by an electric motor delivered high-pressure fuel of Iso-octane to the common rail. Fuel temperature was kept at room temperature using a water-cooled heat exchanger in the fuel circulation from the fuel tank to the common rail, then back to the fuel tank.

Figure 1 shows the optical setup of the PIV measurement. The TSI PIV system consists of a Pegasus-PIV laser, a set of laser sheet formation optics, a Photon FASTCAM-APX RS high-speed video camera system and INSIGHT 3G PIV image analysis software. The double-head Nd:YLF laser produces green light at a wavelength

of 527 nm with a beam diameter of 1.5 mm. It has the ability to operate at the repetition rate of 10 kHz with a total power of 10 watts per head. Energy per pulse is 10 mJ and the laser pulse width is less than 180 ns at 1 kHz repetition rate per head. The energy stability is high with the rms of less than 1% in the laser power. The double cavities of the Pegasus-PIV laser are triggered independently by a laser pulse synchronizer, therefore the time delay between the two double pulses can be set much smaller than that of the repetition rate. Synchronised with the Pegasus-PIV laser was a Photon FASTCAM-APX RS high-speed video camera system capable of recording up to 3000 fps with the full resolution of 1024 x 1024 pixels per frame.

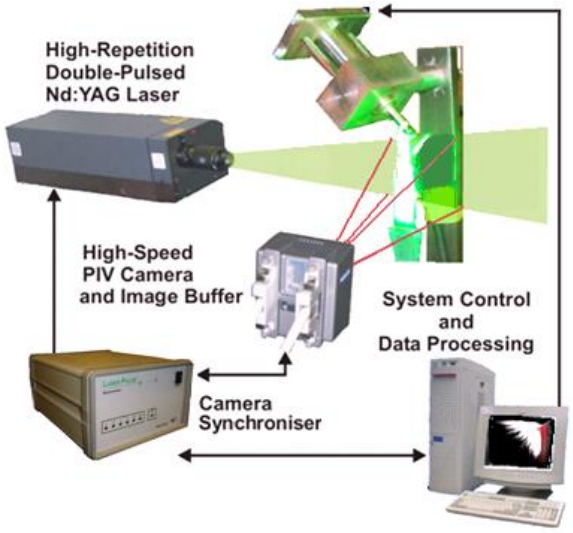


**Figure 1** Experimental setup of the high-speed PIV system

In the two-dimensional spray visualisation study, the diode pumped Nd:YLF laser was replaced by a 1.5W Argon-Ion laser which provided continuous illumination for spray visualisation. The same Argon-Ion laser was part of the DANTEC PDA system, which was used for the LDV measurement in this study.

## Results and Discussion

Vortex structures demonstrated by the fuel droplet movement and re-distribution are revealed after the end of a fuel injection by the 2D Mie scattering visualisation with an aid of a high speed camera. The light sheet, shown in Figure 2, was located at the symmetrical plane of the conical spray. The camera was perpendicular to the light sheet and the speed of imaging was 7200 fps with an exposure time of 90 μs.

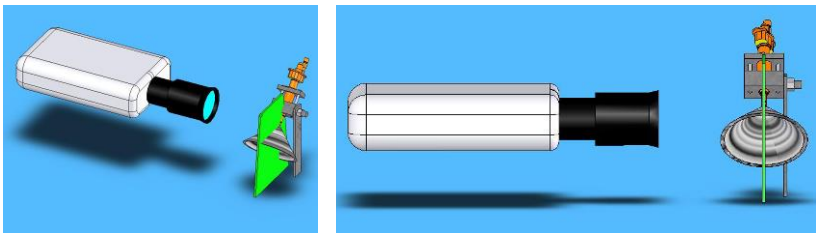

**Figure 2** Setup of Vertical Mie-scattering Visualisation

Figure 3 shows the evolution of a spray. The nominal cone angle of the spray of this injector was close to 90°. The axis of the injector was tilted 45° to the gravitational vertical so that the in-plane spray cone edges are in horizontal and vertical directions. Previous studies of conventional spray visualisation have shown that the hollow cone of the spray following the annulus nozzle passage was disintegrated into a string structure. The string structure of the spray is evident in the images of Figure 3 between 0.11 ms and 0.53 ms. This was during the spray injection with the injection duration of 0.6 ms; the light scattered by the fuel droplets in liquid phase acted as a secondary illumination, so that the front surface of the spray can be unintentionally visualised and the string structure can be identified. At 0.53 ms, a recirculation ring was observed outside the spray. The

recirculation area grew with time and formed a ring of vortex outside of the conical spray, as shown in the image of 1.09 ms; referred to as outer vortex. This ring of vortex has a counter rotating ring of vortex inside the spray; referred to as inner vortex. The inner ring of vortex became clear in the image at 1.64 ms. As the injector needle was closed, fuel droplets from upstream near the injector nozzle were observed drawn into these rings of vortices. Those fuel droplets became the tracing particles for flow visualisation and for the PIV measurements later on. Although the vortices at the two sides of the injector axis are not exactly symmetrical, but the centres of the two main vortex rings in the visualisation plane are symmetrical about the injector axis, indicating that the two counter rotating vortex rings were formed simultaneously inside and outside following the conical shape of the spray. In the images from 1.09 ms onwards, the vortices grew in size with time showing the dissipation of the vortices and at the same time, the flow was losing its tracing particles as fuel droplets evaporated. It should be pointed out that the circular structures of fuel distribution with dark centres in a single image do not represent vortices at the time, as they could be formed at an earlier stage of the injection due to either the instability of the spray or the spray induced vortices. The two main vortex rings marked in Figure 3 are the result of the observation of consecutive images of the recording.

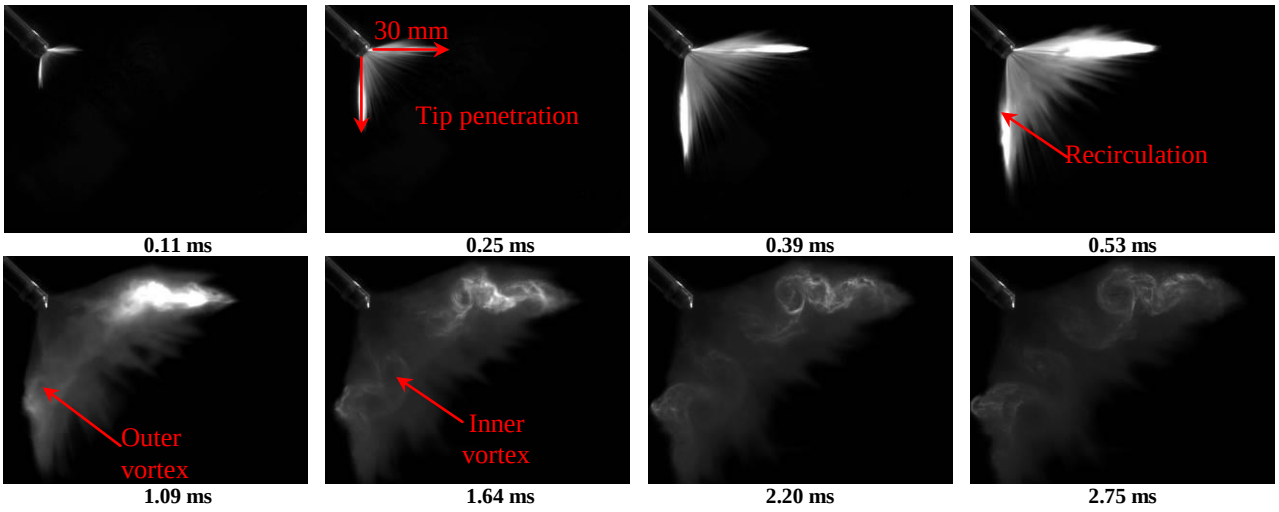


**Figure 3** 2D Mie Scattering Images of Spray Evolution
(Injection Pressure 200bar and Injection Duration 0.6 ms)

In Figure 4, the injection pressure was kept constant at 200 bar and injection durations were 0.6 ms, 1 ms and 2 ms. Figure 4 (a) shows the raw images of the sprays at around 1.1 ms ASOI. This particular imaging time was chosen to show clear differences between the three injection durations. At this time, injection was definitely completed for the injection duration of 0.6 ms and it was in the middle of the injection for the injection duration of 2 ms. As for the injection duration of 1 ms, the injector needle was just closed, but the string structure of the spray was still visible. The three images of injection durations of 0.6, 1 and 2ms show clear geometrical similarities in terms of the location of the recirculation and the spray tip penetration.

Figure 4 (b) shows the spray tip penetration as illustrated in Figure 3 at 0.25 ms. The tip penetration is defined as the furthest distance of the spray from the injector exit. In each image, a vertical penetration and a horizontal penetration distance were measured by a computer program with a fixed threshold for all three cases of injection durations. The horizontal and the vertical penetration were found advancing at the same rate at the beginning until the penetration of the spray reached around 35 mm, shown as the initial linear part of the graph. The averaged penetration speeds over the two sides and the three cases is 115 m/s with 2% variation in the injection durations of 0.6, 1, and 2 ms. After the linear part, both horizontal and vertical penetrations were slowed down considerably with the horizontal penetration advanced further compared to the vertical side. Comparing the vertical penetrations of the three injection durations, marked by hollow symbols in Figure 4 (b), no clear difference in the vertical penetrations was found in the three injection durations. Spray droplets after EOI in a shorter injection duration of 0.6 ms or 1 ms carried on moving away from the injector at a same speed as those in the injection duration of 2 ms, which were in the middle of injection until 2 ms. There was a slight difference in the horizontal penetrations, marked by solid symbols in Figure 4, the increase in the injection duration resulted a higher penetration length after the linear part of the graph, however the limits of the penetrations were not changed much in the three cases. The results also show that at the end of injection the average penetration speeds in vertical direction for three injection durations were found between 10 to 12 m/s, whereas in the horizontal

direction the penetration speeds were in the range between 14 to 21 m/s for the three injection durations. Penetrations on both sides show a massive reduction in droplets momentum compare to those in the beginning of the injection which is due to considerable secondary breakup taken place in the early part of injection producing smaller droplets and therefore their loss of momentum and penetration; more details can be found in [8] where the variation of Webber number, We, with distance from injector are discussed and shows massive reduction in We within the first 10 mm from the injector.

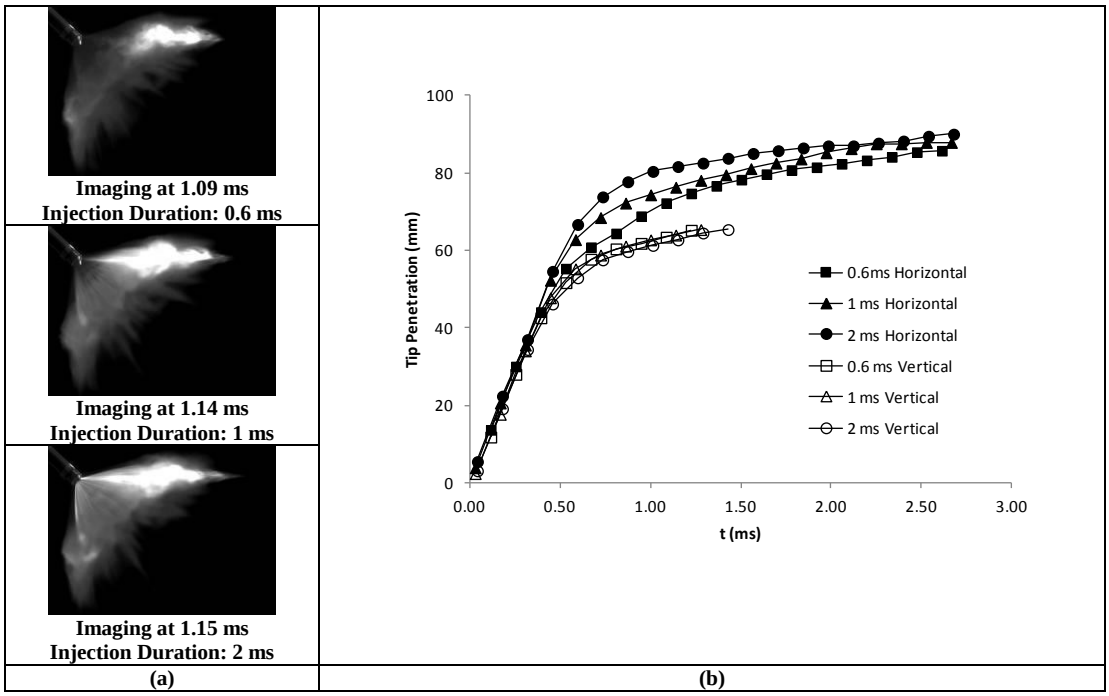


**Figure 4** (a) Spray Visualisation (b) Spray Penetration (Injection pressure 200 bar)

As mentioned earlier, a static image of the 2D Mie scattering of fuel droplets is unable to show the velocity field of the vortices in the wake of an injection. This information was obtained by the PIV technique using the floating fuel droplets as tracing particles for the air/fuel droplet two-phase flow. Figure 5 shows the instantaneous velocities in the wake of sprays, which are superimposed on one of the two processed PIV images used for obtaining the velocity vectors. The laser sheet was projected towards the spray from left to right in the images. In the areas where no sufficient scattered light existed, the PIV measurements were not available and only one half of the images were processed and presented for the PIV measurements. Due to the restriction of the PIV sampling rate, maximum 1500 pairs per second with the full spatial resolution, the PIV results in Figure 5 are snap shots of different injections.

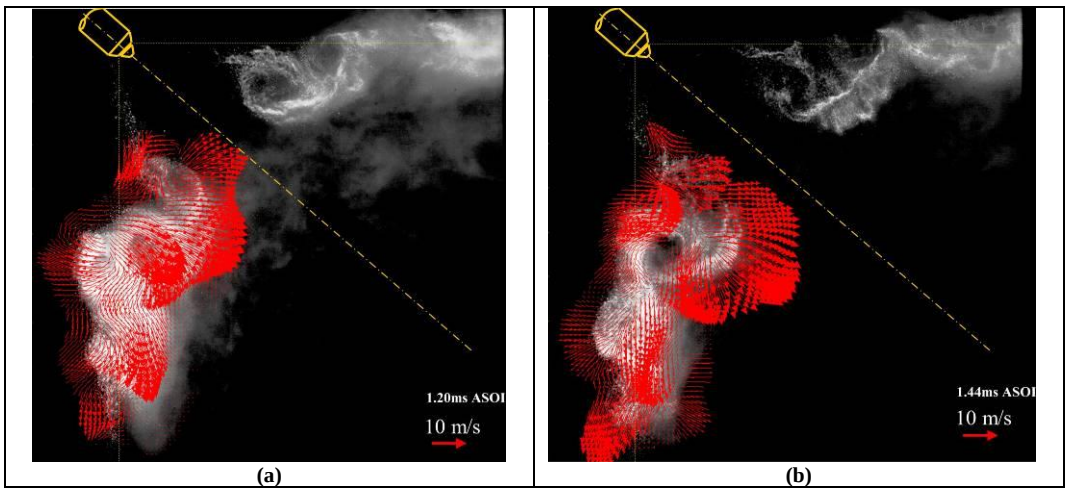

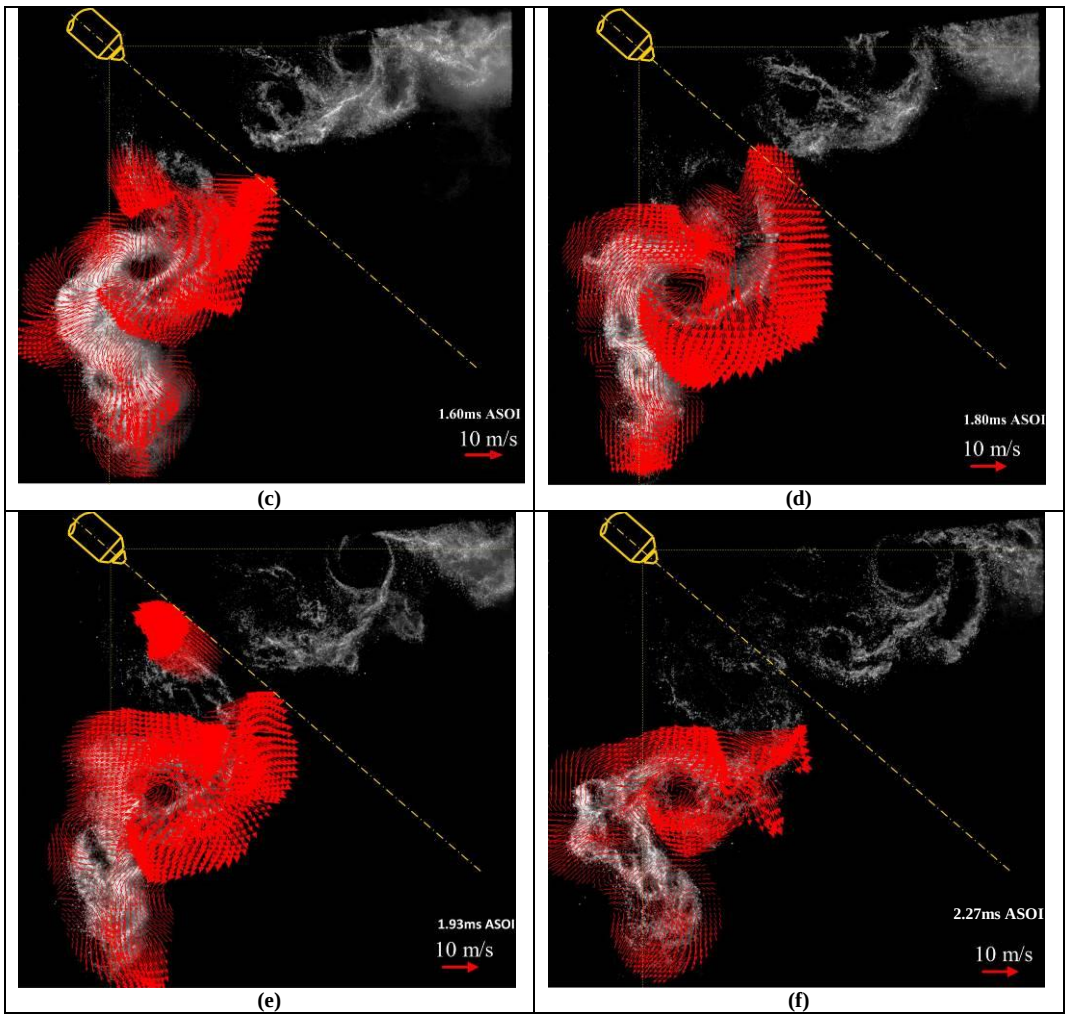


**Figure 5** PIV Measurement of Recirculation Zones
(Injection Pressure 200bar and Injection Duration 0.6 ms)

The velocity fields presented in Figure 5 show the effect of the mutual interaction of the two counter rotating vortices, generating a flow directed into the spray cone. The sequence of images show the expansion of the vortices radially toward the axis of the injector at 1.20 ms ASOI and onwards, which can be verified by what was observed in the 2D Mie scattering visualisation. In the 2D Mie scattering visualisation, focus of the study was on the formation of vortices shown in the images, whereas the PIV results show that the radial expansion is the dominant feature of the velocity field.

In addition to radial expansion of the vortices, the rotation of the vortices was also superimposed on translation movement of the vortices, especially before 1.60ms ASOI. When a translation velocity is superimposed on the relative rotational velocity field, it shifts the location of the zero velocity perpendicularly to the translation velocity. The translation velocity decreased with time as that of the spray tip penetration. At 1.60ms ASOI, it can be observed that the centre of velocity field of the outer vortex did not coincide with the centre of the background image. It was estimated the outer vortex moved towards the injection jet direction with a sliding velocity of around 10 m/s.

Because of the rotation of the inner vortex ring, an upward flow was built up in the upper central region of the spray cone. In the image at 1.93ms ASOI, fuel droplets were found moving up towards the injector tip with velocities about 15 m/s, indicating a strong upward flow in this region. Finally, at 2.27ms ASOI the centre of the velocity field is almost overlapped to the fuel distribution vortex image, which means that the translating speed was significantly reduced or in other words the vortex at this stage did not move any further.

The instability in the spray has been demonstrated in terms of the breakdown of annular spray film into a number of strings, a wavy surface along a string, flapping in spray cone angle, formation of recirculation around the spray and variation in the spray front penetration[7]. Figure 5 shows the instantaneous velocity distributions of

fuel droplets. Although a pair of vortices is clearly identified after the end of injection, the original start of the outer ring of vortex can be traced back to the recirculation developed at the out surface of the spray during an injection. Individual snap shorts of the flow field show the repeatability in the occurrence of vortices generated by the spray. However the repeatability in the formation of vortices is much less evident due to the instability in both spray dynamics and aerodynamics. No attempt was made to obtain an ensemble average over a number of sprays in this study.

In the application of the gasoline direct injection engines, in-cylinder air flow and fuel droplet distribution are the main factors which affect the air/fuel mixture formation for achieving repeatable and reliable combustion in every single engine combustion cycle under a wide range of engine operation condition of load and speed. Results of instantaneous velocity distributions will be useful for understanding the time averaged flow measurements by other laser diagnostic techniques, such as LDV or PDA, as well as for interpreting CFD results. In addition, a single shot image of a flow field gives the information on what happened in a real flow.

The PIV analysis using fuel droplets as tracing particles was successful where the interrogation area was away from the injector nozzle and when it was after EOI. In the vicinity of the injector tip, no fuel droplets were present for PIV analysis, whereas during a spray injection, fuel droplets were too dense to be distinguished by an imaging based optical technique. Extra seeding particles were introduced in order to overcome the lack of tracers of naturally existing fuel droplets. For the same experimental setup, shown in Figure 1, the area around a spray was seeded with atomised water droplets with sizes of order of 2 μm and a mean velocity of 0.3 ± 1.3 m/s, measured by LDV. The air flow is now visible with the seeding droplets, as shown in Figure 6, so it is possible to study air flow during injections. Air flow surrounding the spray is important, especially the velocity component of the air flow towards the spray, as the air entrainment influences the fuel droplet evaporation.

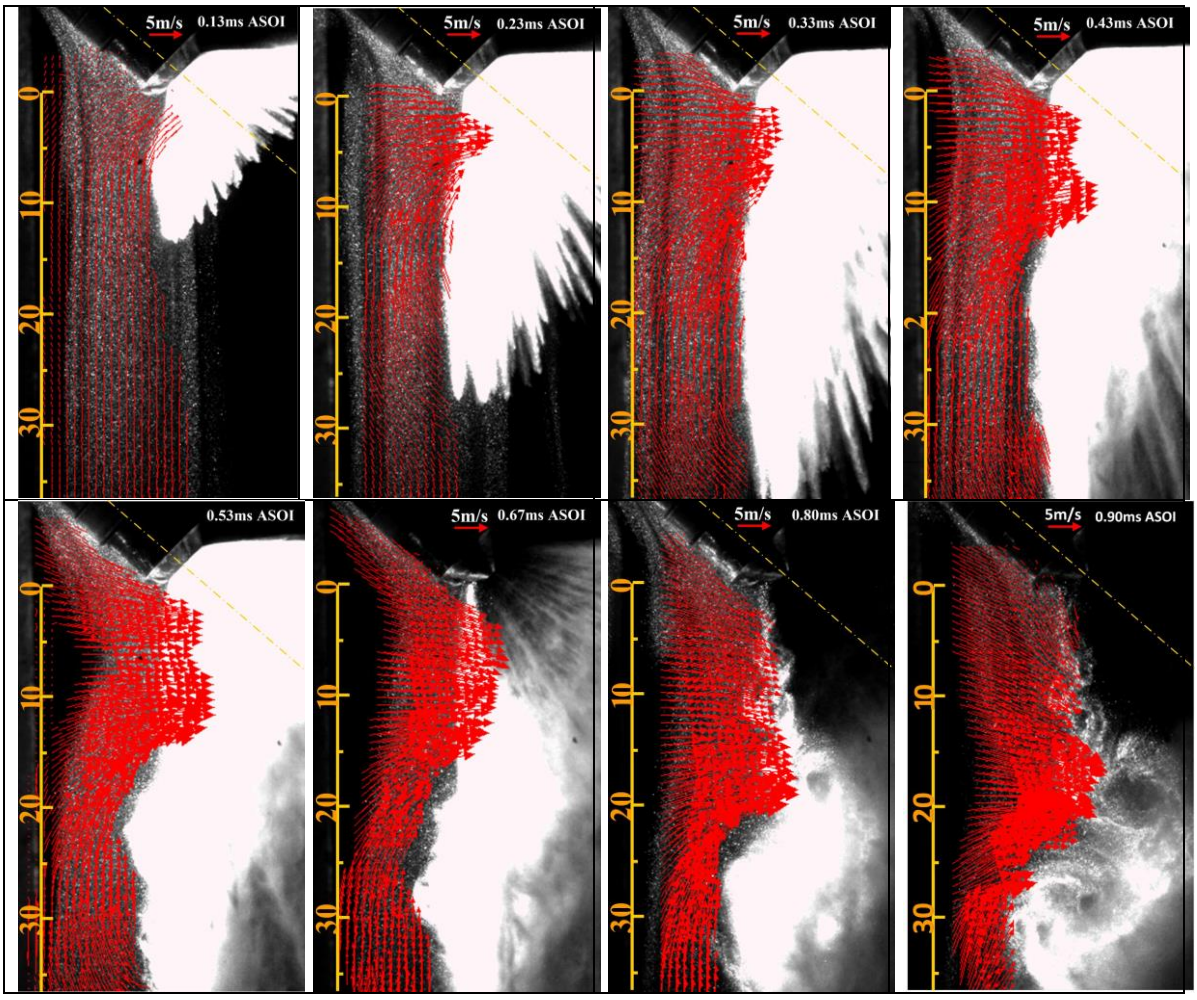


**Figure 6** Air Entrainment
(Injection Pressure 200bar and Injection Duration 0.6 ms)

Figure 6 shows air entrainment as sprays evolved. At 0.23 ms ASOI, the air entrainment exhibited a jet like profile with a peak jet velocity at a distance of about 4 mm from the injector exit and the direction of air flow of at the peak velocity was almost normal to the spray flow. As the spray evolved the horizontal component of the air velocity increased in intensity with values up to 10m/s and hit the spray in the same near nozzle area, but with an expanded effected area on the spray further downstream, so that at 0.33ms ASOI the air entrainment in the form of an air jet was found in the area up to 8mm away from the nozzle exit. At 0.43ms ASOI, the onset of the outer recirculation can be seen at a distance of about 10-15mm from the nozzle; in fact, the faint bump on the spray profile represents the initiation of the outer vortex that was discussed in the previous section. At this stage, the air velocity profile becomes wider and takes a shape of double peak jet progressively extending downstream. A broader air jet towards the spray was found at 0.53ms ASOI comparing to that at 0.43ms ASOI.

From 0.67 ms ASOI onward the PIV images clearly show how the air entrainment follows the evolving outer vortex ring promoting its formation with a horizontal velocity of about 10m/s preceding its motion. Finally, at 0.30ms after the end of the injection (or 0.90 ms ASOI), the spray starts loosing its density and therefore it is possible to visualise the internal cross-section of the spray and the full set of counter rotating vortices as was previously shown in Figure 5. The last image at 0.9ms ASOI, also reveals how the air entrainment is interacting on the wakes of sprays and more specifically on the inner vortex, which explains its displacement toward the injector axis at a later stage shown in Figure 5.

The PIV measurement was validated by a LDV measurement. The measurement location, the control volume of the beam crossing, was set close to the injector nozzle exit. Due to the restriction of access, the air flow speed in the direction towards the spray was measured at a location above the spray. Its axial symmetrical location in the area of the vertical side of the spray is marked as the green dot in Figure 7 (a). The velocity component towards the spray is marked as in x direction. The asymmetrical features of the spray and surrounding air flow exist, but it is of a secondary importance and not considered in Figure 7. Figure 7 compares velocity fields at the vertical side of the spray at a fixed imaging time of 0.23 ms ASOI and temporal velocity variations at one point, of which the relative position to the spray is shown in the graph.

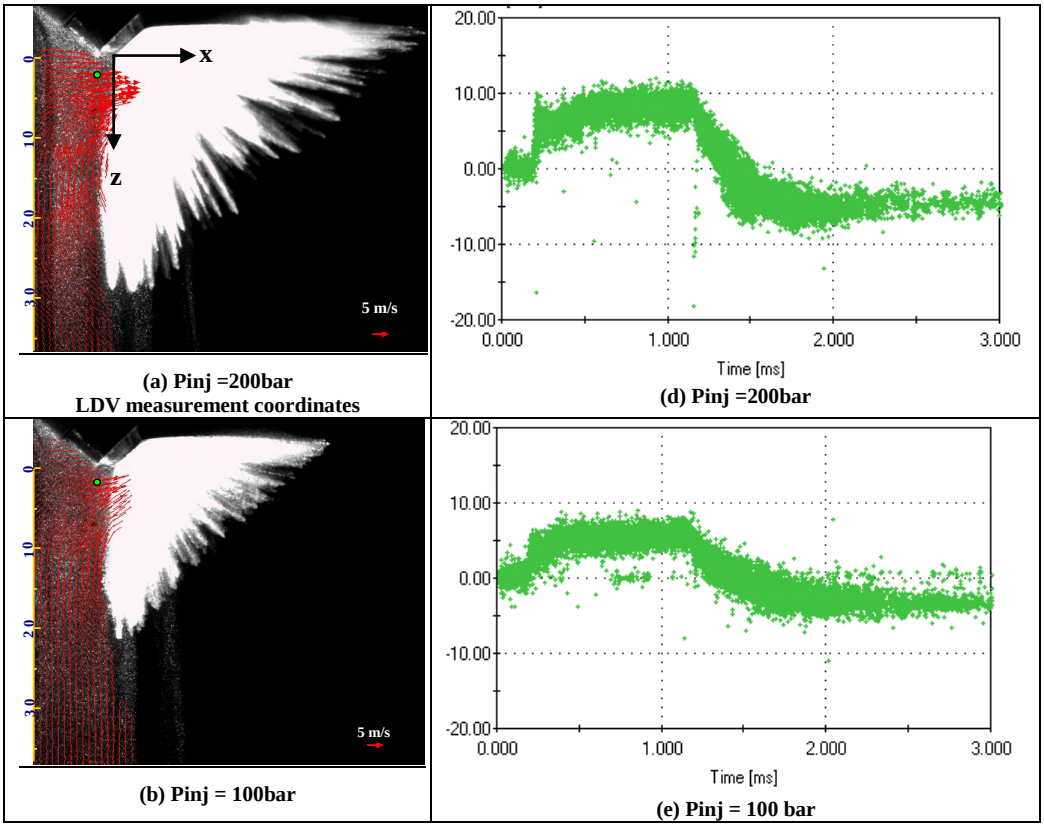


**(a) Pinj =200bar**
**LDV measurement coordinates**

**(d) Pinj =200bar**

**(b) Pinj = 100bar**

**(e) Pinj = 100 bar**

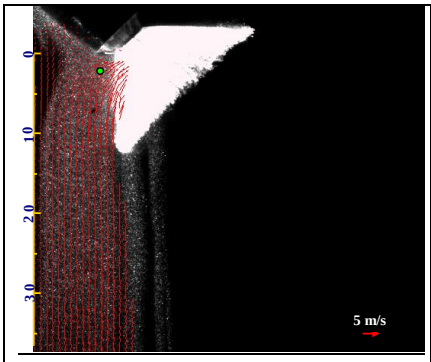


(c) Pinj = 50bar

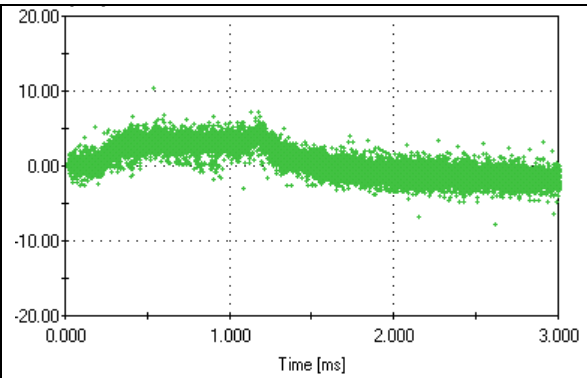


(f) Pinj = 50 bar

(a)-(c) PIV at 0.23ms ASOI

(d)-(e) LDV Vx at CV position x= -1.2 mm, y=0, z=1.2mm

**Figure 7** PIV and LDV Measurements of Air Entrainment

The velocity of the air entrainment was assessed at three injection rail pressures of 200bar, 100bar and 50bar and the results are presented in Figure 7. Each of the three rows in Figure 7 corresponds to an injection pressure. The first column of images represents the PIV velocity field measurements and the second column of graphs shows the temporal variations of LDV measurements for the normal velocity components towards the spray. PIV measurements show the velocity component in the direction towards the spray increased with the injection pressure. At 50 bar injection pressure the velocity was about 2 m/s which increased to 4 and 7 m/s at injection pressures of 100 and 200 bar respectively. The trend of increase in air entrainment velocity with the injection pressure matches with the LDV measurements. The LDV results show the air entrained flow motion exhibited a steady and relatively strong velocity field near the nozzle exit. A step increase in air motion was observed at injection pressures of 100 and 200 bar, whereas the air motion was gradually built up at 50 bar injection pressure. At the injection pressure of 200 bar, instantaneous velocities were found in the range between 5 to 10 m/s. This range was reduced to 3 to 8 m/s at the injection pressure of 100 bar and was decreased further to 1 to 5 m/s at 50 bar of injection pressure.

The agreement in the PIV and LDV measurements verified that the setup of the PIV technique, including the seeding density in the range of 20-30 per interrogation area, was adequate in the study of air entrainment. In the spray recirculation measurements the particle density depended on the number of spray droplets, which was around 10 droplets per interrogation area to produce a valid result. The maximum displacement of particle images was set to be about one eighth of the interrogation window size to reduce the measurement uncertainties caused by particles leaving/entering the interrogation area and sub-pixel values were used in the cross-correlation to increase the measurement accuracy.

## Conclusions

An experimental investigation was carried out to characterise the fuel spray structure at the end of injection and the induced air-entrainment near nozzle exit of a pintle-type injector using two-dimensional Mie scattering imaging, PIV and LDV techniques. The followings are the most important findings:

- A pair of count rotating vortices was identified by the two-dimensional Mie scattering after the end of injection. The recirculation zone formed by vortices trapped fuel droplets to propagate further away from the injector tip.

- Using the fuel droplets as the natural seeding for Particle Image Velocimetry (PIV), velocity fields were obtained to provide the speeds of fuel droplets in the vortices in the recirculation zone. The results provided an overview of quantitative instantaneous velocity fields and flow stream patterns, which will be useful for understanding the fuel transportation, as well as for CFD validations in the prediction of spray characteristics of the outwards opening pintle-type Injectors.

- PIV and LDV measurements of air motion induced by the spray show the degree of air entrainment which is vital for the phase change of fuel evaporation.

## Acknowledgements

The financial and technical support provided by BMW AG is gratefully acknowledged. The authors would also like to thank Tom Fleming and Jim Ford from City University London for their valuable technical support during the experimental programme.

## References

[1] 1. Nouri, J.M., Hamid, M.A., Yan, Y. and Arcoumanis, C., *Spray characterization of a piezo pintle-type injector for gasoline direct injection engines* Journal of Physics: Conference Series, 2007. **85**(ICOLAD 2007).

[2] 2. Befrui, B., Corbinelli, G., Robart, D., Reckers, W. and Weller, H., *LES simulation of the internal flow and near-field spray structure of an outward-opening GDI injector and comparison with imaging data.* SAE paper, 2008: p. 01-0137.

[3] 3. Wigley, G., Pitcher, G., Nuglisch, H., Helie, J. and Ladommatos, N. *Fuel spray formation and gasoline direct injection*. in *8th International Symposium on Internal combustion diagnostics (AVL)*. 2008. Baden-Baden, Germany.

[4] 4. Zigan, L., Schmitz, I., Flügel, A., Wensing, M., & Leipertz, A. , *Structure of evaporating single-and multicomponent fuel sprays for 2nd generation gasoline direct injection.* Fuel, 2011. **90**(1): p. 348-363.

[5] 5. Martin, D., P. Pischke, and R. Kneer., *Investigation of the influence of multiple gasoline direct injections on macroscopic spray quantities at different boundary conditions by means of visualization techniques.* International Journal of Engine Research, 2010. **11**(6): p. 439-454.

[6] 6. Marchi, A., Nouri, J. M., Yan, Y. and Arcoumanis, C., *Internal flow and spray characteristics of pintle-type outwards opening piezo injectors for gasoline direct-injection engines.* SAE Trans. J. Engines, 2007. **116**(3): p. 01-1406.

[7] 7. Marchi, A., Nouri, J., Yan, Y. and Arcoumanis, C., *Spray stability of outwards opening pintle injectors for stratified direct injection spark ignition engine operation.* International Journal of Engine Research, 2010. **11**(6): p. 413-437.

[8] 8. Marchi, A., *Internal flow and spray characteristics of an outwards opening pintle-type gasoline-injector*. 2009, City University London.